Intelligent Inspection Robotic System for Bridge Cable Defect Identification and Positioning

Jie Li [1,2], Beibei Li [3], Chunlei Tu [1], Mengqian Tian [1], Xingsong Wang [1]

[1] School of Mechanical Engineering, Southeast University, Nanjing 211189, China

[2] College of Automation, Nanjing University of Posts and Telecommunications, Nanjing 210003, China

[3] NO.703 Research Institute of CSSC, Harbin 150028, China

xswang@seu.edu.cn

Abstract. With a large number of cable-stayed bridges being built and applied, these cables need regular inspection and maintenance to ensure traffic safety. Cable inspection robots can effectively replace traditional manual detection, and the rapid identification of defects is very important to improve inspection efficiency. This paper proposes an intelligent robotic system for bridge cable defect identification and positioning. The 360-degree cable surface images are captured simultaneously by four cameras installed around the developed inspection robot. Based on the Mask R-CNN and image processing, the robotic system can quickly identify the surface defects of cables. The deep learning network is mainly composed of multiple layers of convolutional neural networks, which can achieve classification, regression and pixel-level mask generation of cable surface defect objects. The location information of these identified cable defects will be measured and recorded by ultra-wide band (UWB) positioning components. These positioning data are sent to Kalman filter for optimal estimation. Experimental results indicate that the inspection robotic system can successfully and quickly identify cable defects, and the average processing speed of each cable image is about 0.16s. The robot can realize high-precision defect positioning, and the positioning error is within ±2cm. The application of the robotic system is conducive to confirming the safety of bridges, improving the efficiency of cable inspection, and providing support for the subsequent maintenance.

Keywords: bridge maintenance, deep learning, inspection robot, defect identification

1. Introduction

The massive construction of bridges makes transportation more convenient, and cable-stayed bridges are an important and widely used form of bridge structures. Cable-stayed bridge is a combined system composed of three major parts: tower, beam and cable. The stay cable is anchored on the tower and the beam to provide multi-point elastic support for the main bridge beam, which greatly reduces the bending moment of the main beam and improves the spanning capacity of the bridge. However, after a long period of use, the stay-cable may be defective and damaged. Regular inspection of bridge cables is an important method to ensure the safe use of bridges. Because cable inspection is a high-risk, time-consuming and costly task, traditional manual inspection has been unable to complete the rapid inspection of large bridges. The safety of the bridge cable needs to be guaranteed in time, which is in urgent need of automated equipment instead of manual completion.

The specialized climbing robot [1,2] has become an important automatic detection method, which can accomplish shuttle running on cables. Since the operating environment is a very long steel cable, climbing robots are more practical and convenient than aircrafts. Climbing robots can be equipped with different equipment and instruments to identify, clean, and repair cable defects.

Most cable defect identification methods of inspection robots are limited to remote video monitoring. Manually identifying cannot real-time find all defects and the workload is very huge. In recent years, some automatic cable defect detection was completed through image processing methods [3]. However, the recognition results of these methods are not accurate enough, and they are easily interfered by the surrounding environment. As an emerging artificial intelligence method, deep learning can achieve more accurate classification and regression by applying convolutional neural networks. Some networks have been developed for image classification, such as VGGNet [4], ResNet [5], SSD, YOLO, and Faster R-CNN [6].

Since the cable inspection robot is working at height, it is necessary to locate the robot to determine the position of the cable defect. The common method is to record the mileage information through encoders, but generated cumulative error is very large after running a long distance. When robot's wheels slip or cross obstacles, the mileage information will be inaccurate, which directly affects the robot's positioning. As a positioning technology, UWB technology has been applied in many aspects [7,8]. Relative to mileage positioning, the absolute position information calculated by UWB method has better stability. Through algorithm optimization, UWB positioning in plane or space has been greatly improved [9].

In this paper, we propose an inspection robotic system for cable defect identification and positioning. The cable inspection robot with elastic suspension and V-shaped wheels was designed, which can climb smoothly on bridge cables. The cable surface images can be captured by four cameras installed around the robot. Based on Mask R-CNN, the robotic system can not only achieve classification and bounding box regression to defective objects, but also further accomplish the pixel-level instance segmentation. In order to locate cable defects more accurately, UWB components are used to measure robot's running distance. Meanwhile, UWB data are sent to Kalman filter for optimal estimation. Some experiments of cable defect identification and positioning were carried out to verify the stability and feasibility of the inspection robotic system.

2. Cable Inspection Robotic System

2.1. Inspection Robot

As an important part of cable-stayed bridges, cables provide great tension to bridge decks, and their length can reach several hundred meters. The main purpose of the cable inspection robot is to climb smoothly on cables of different diameters. As shown in Fig. 1, the developed cable inspection robot is composed of two driving wheels, two driven wheels, two motors, an adjustable robot frame, four elastic suspension mechanisms, four anti-deviation mechanisms and four cameras. The driving wheels and driven wheels are V-shaped wheels, which can achieve maximum fit on the cable surface and provide greater friction for the robot. The motors and driving wheels are connected by a gear transmission system, its transmission ratio is 2:1.
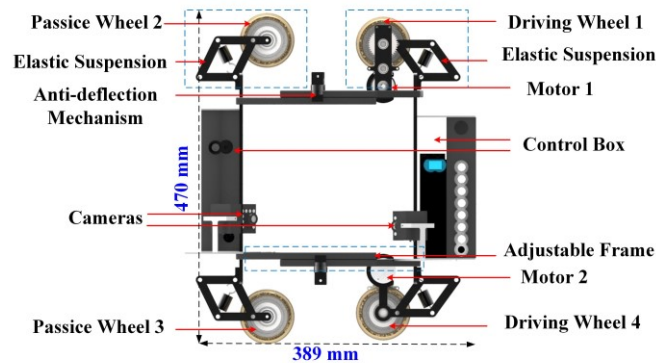
Fig. 1: Cable inspection robot with elastic suspensions.

The elastic suspension mechanisms are designed and installed on four V-shaped wheels, which include quadrilateral links, springs and rotating shafts. These springs provide sufficient tension force for elastic suspensions, which can tightly press V-shaped wheels on the surface of cables. Anti-deflection mechanisms are installed in the middle of the robot frame, which is used to prevent the robot from deviating from the cable during climbing. Through the adjustable robot frame, the inspection robot can clamp the cables of different diameters (from 50 to 230 mm).

Four cameras installed around the robot frame are used to capture images of cable surfaces. The position of the cameras relative to cable surfaces can be adjusted by telescopic mechanisms. In order to collect clear and complete cable surface images, camera angle and distance need to be adjusted according to cable diameter. Four acquired images need to meet the following requirements:

(1) These cable surface areas acquired by four cameras should be overlapping to ensure no missing.

(2) The proportion of the cable object in four images should be greater than 50% to ensure that cable surface images are clear.

Fig. 2 shows the position diagram of four cameras of the cable inspection robot, their positions are symmetrical. Take a camera as an example to analyze camera positional relationship, the distance between the camera and the cable surface is d, the diameter of the cable is R, the minimum imaging distance of the camera is r, and the angle from the camera to the cable edge is θ. We can get:
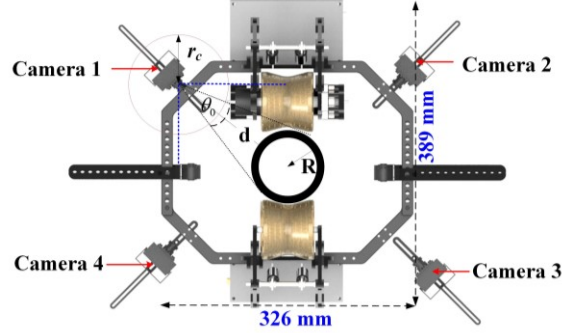
Fig. 2: Camera distribution of the cable inspection robot.

$$d > r \tag{1}$$

When the proportion of the cable object is greater than 50%:

$$\theta_0/2 < \theta < \theta_0 \tag{2}$$

where θ_0 is the maximum imaging angle of cameras.

By analyzing geometric relations:

$$\sin\frac{\theta}{2} = \frac{R}{d+R} \tag{3}$$

The distance d should meet the following equation:

$$\frac{R}{\sin\frac{\theta_0}{2}} - R < d < \frac{R}{\sin\frac{\theta_0}{4}} - R \tag{4}$$

When θ_0 is 100°, R is 50 mm and 230 mm, the corresponding camera distance d should be set as:

$$\begin{cases} 70.2mm < d < 314mm \quad (R = 230mm) \\ 15.2mm < d < 68mm \quad (R = 50mm) \end{cases} \tag{5}$$

2.2. Control and Identification System

As shown in Fig. 3, the robot control and identification system includes motion control components, UWB positioning components, an image splitter, a wireless image transmission device, a remote-control unit and a remote computer. Motion control components can drive the robot to climb along bridge cables through two motors. The image splitter merges four cable surface images into an image, and the wireless image transmission device sends it to the remote computer. The UWB positioning components record the robot's real-time position by calculating the distance between the robot's UWB tag and the UWB anchor on initial position, as cable defect position data.

As a terminal device for data analysis and processing, the remote computer will undertake communication with the cable inspection robot, cable defect identification, and image processing. The remote computer is equipped with a RTX2070 GPU, which accelerates deep learning training and cable defect identification. Combines with UWB positioning data, the remote computer also estimates the position of cable surface defects.
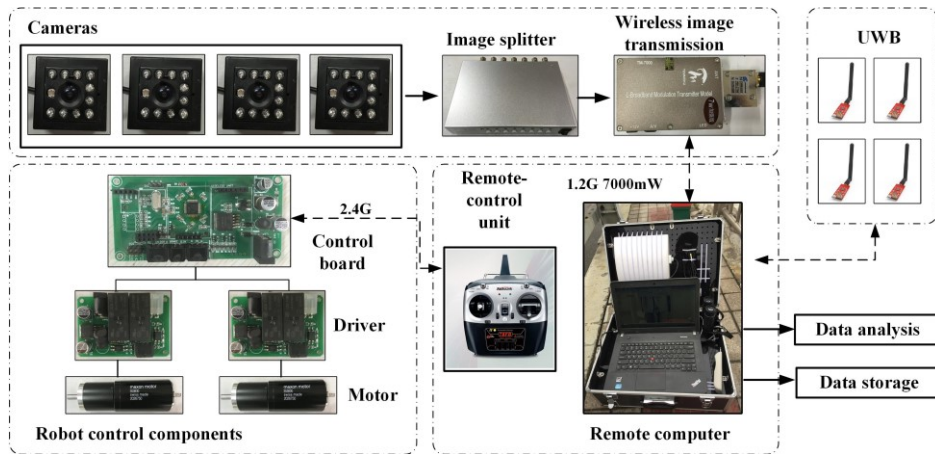
Fig. 3: Robot control and identification system.

3. Identification of Cable Defects

3.1. Identification Method

After a long period of open-air work, bridge cables may generate some defects on their surface, which directly affects the safe use of bridges. These cables have irregular shape defects and different degrees of damage [10]. There may be some dirt and rust on cables, which leads to the popular image processing unable to make accurate prediction, and cannot confirm defect's size. Image processing is more susceptible to lighting adjustment, and the deep learning network can solve the problem of defect image interference.

The ultimate goal of the robotic system is to obtain cable defect position and make damage analysis. Deep learning networks are used to accurately segment defect targets. Fig. 4 shows the basic process of identifying and extracting cable surface defects. In the initial stage, the robot captures 360-degree cable images through four cameras. Multilayer neural networks are used to identify cable defects and make image instance segmentation, which is Mask R-CNN [11]. After acquiring cable defect images, a series of image processing are performed to analyze the damaged condition and fuse the position information.
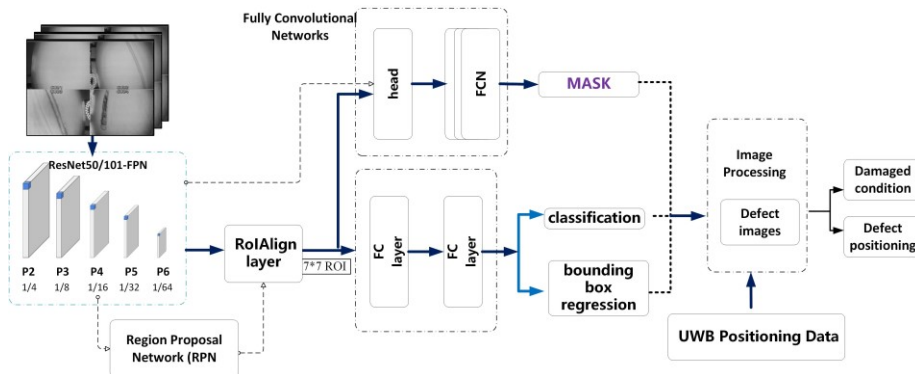
Fig. 4: Deep learning framework for cable defect identification.

The process of Mask R-CNN for defect identification mainly includes two stages: the first stage is the generation of candidate regions, which mainly includes feature extraction by convolutional neural networks, Region Proposal Network (RPN) and RoIAlign layer [12]; the second stage is the classification and regression of objects, and mask generation.

At the beginning, convolutional neural network layers (such as ResNet50 and ResNet101) are used to extract feature maps of cable images. Deeper convolutional neural networks can extract deeper features of cable defect images, but that will ignore the features of small-sized objects. In the defect feature extraction stage, Feature Pyramid Networks (FPN) [13] is used to fuse the feature maps from the bottom layer to the high layer, which fully utilizes the features of different depths.

The feature map extracted by ResNet50/101-FPN will be transferred to RPN. The purpose of RPN is to recommend region of interest (ROI) to the network. It is a fully convolutional network that extracts features from the original image. In order to avoid deviation caused by RoI pooling layer, the obtained region proposals are sent to RoIAlign layer without quantization. After RoIAlign pooling layer, on the one hand, ROI connects two fully connected layers for image classification and bounding box regression.

The deep learning networks finally outputs three branches for cable defect images: classification, bounding box regression and mask prediction branch. The classification layer determines the category of the object. The box regression layer improves the position and size of the bounding box. The mask branch uses FCN [14] to segment objects in images by pixels, and predicts $m \times m$ masks from each ROI. In the dataset for defect identification, the number of categories is 2 (background and defect), and the output network is simpler (depth 2).

3.2. Training

During the training process, the loss function is defined as:

$$L = L_{rpn} + L_{Mask} \tag{6}$$

$$L_{rpn} = L_{cls} + L_{loc} = \frac{1}{N_{cls}}\sum_i L_{cls}\left(p_i, p_i^*\right) + \lambda_1 \frac{1}{N_{reg}}\sum_i p_i^* L_{reg}\left(t_i, t_i^*\right) \tag{7}$$

$$L_{Mask}\left(p_i, p_i^*, t_i, t_i^*, s_i, s_i^*\right) = \frac{1}{N_{cls}}\sum_i L_{cls}\left(p_i, p_i^*\right) + \lambda_2 \frac{1}{N_{reg}}\sum_i p_i^* L_{reg}\left(t_i, t_i^*\right) + \gamma_2 \frac{1}{N_{mask}}\sum_i L_{mask}\left(s_i, s_i^*\right) \tag{8}$$

The loss function includes RPN network loss L_{rpn} and mask prediction loss L_{Mask}, which is related to classification, regression, and mask prediction of cable defects. The defintion of L_{Mask} allows the networks to generate masks for every category without competition. L_{Mask} is only defined on the **k**-th mask.

The training dataset includes 300 cable images with defects. The input size of images is 640×480 pixels. Under the conditions of satisfying defect imaging, the smaller image size helps speed up training and identification. There are many types of defects, and the defect outline was clearly depicted through multiple points during the labeling phase.

In the deep learning training process of cable defect images, the network weights are learned through iterative calculation. The loss function curve changes as shown in Fig. 5. During 1000 steps (iterative computing), the loss function curve rapidly decreases and stabilizes at 0.2-0.3. Due to the use of the latest machine learning library, the training time is greatly reduced and excellent identification results are obtained. Comparing accuracies of 300, 500, 700 and 1000 steps, we found that the training effect after 700 steps is already good and basically stable, and the accuracy is 0.949. Faster training speed helps to improve and optimize deep learning networks for identifying cable defects.
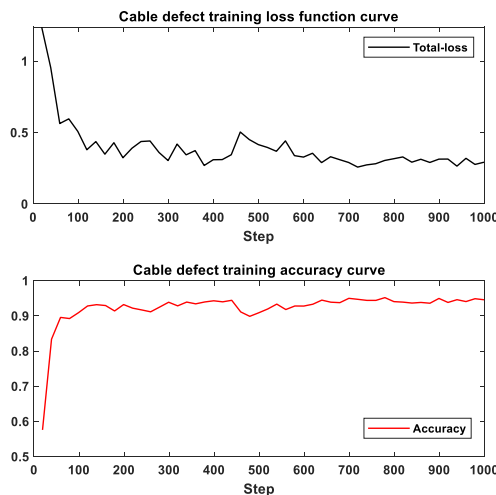
Fig. 5: Loss function and accuracy curve of training cable defect dataset.

4. Positioning of Cable Defects

4.1. Distance Calculation

Robot running distance can be calculated by the encoders on the wheels, but this estimation method produces a large cumulative error. When the robot slips or moves back and forth on cables, the calculated mileage data will no longer meet the actual positioning requirements. UWB positioning components can calculate the position of the inspection robot on the cable by flight time.

UWB positioning components are composed of a UWB anchor and a robot UWB tag. The UWB tag is installed on the robot, and the UWB anchor is placed at the fixed starting position of the tested cable. The flight distance of the signal can be calculated by two way-time of flight (TW-TOF) method [15]. However, since the UWB anchor and the robot UWB tag use independent clock sources, and these clocks have a certain deviation. With multiple signal processing and clock offset increases, the flight time error will continue to increase, thereby making distance measurement inaccurate. We use an improved Double-sided Two-way Ranging (DS-TWR) [16] algorithm to solve this problem. Fig.6 shows the time chart of DS-TWR algorithm.
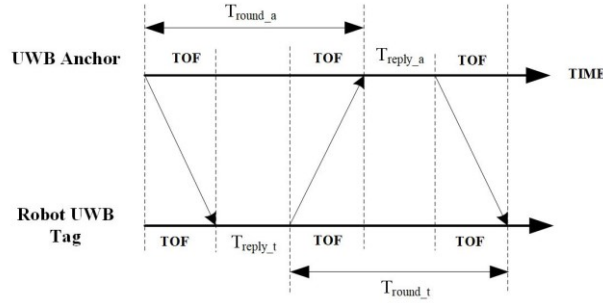
Fig. 6: Time chart of DS-TWR algorithm.

TOF can be calculated:

$$TOF = \frac{T_{round\_a} T_{round\_t} - T_{reply\_t} T_{reply\_a}}{T_{round\_a} + T_{round\_t} + T_{reply\_t} + T_{reply\_a}} \tag{9}$$

In the process of calculating UWB flight time, it is assumed that the clock drift of devices is e_a and e_t, and the observed flight time is:

$$\hat{T}OF = \frac{T_{round\_a}(1+e_a) \times T_{round\_t}(1+e_t) - T_{reply\_t}(1+e_t) \times T_{reply\_a}(1+e_a)}{T_{round\_a}(1+e_a) + T_{round\_t}(1+e_t) + T_{reply\_t}(1+e_t) + T_{reply\_a}(1+e_a)} \tag{10}$$

The flight time error T_{error} is:

$$T_{error} = \hat{T}OF\text{-}TOF = \frac{e_a + e_t + e_a e_t}{2(1+e_a)(1+e_t)} \hat{T}OF \approx \frac{e_a + e_t}{2} \hat{T}OF \tag{11}$$

Since e_a and e_t are far less than 1, the time error is relatively small, and this has little effect on robot distance measurement.

4.2. Optimal Estimate

Kalman filter is used to further improve the robot positioning accuracy. The UWB positioning data has some fluctuations and unsteadiness in real-time dynamic positioning. The state equation and measurement equation of the robot are as follows:

$$\begin{cases} \mathbf{X}_{k+1} = \mathbf{A} \cdot \mathbf{X}_k + \mathbf{B} \cdot \mathbf{U}_k + \mathbf{W}_k \\ \mathbf{Z}_k = \mathbf{H} \cdot \mathbf{X}_k + \mathbf{V}_k \end{cases} \tag{12}$$

where $\mathbf{X}_k = [d_k, v_k]^T$ is the state estimate at time k, d_k represents robot's position, and v_k represents robot's velocity. $\mathbf{A}$ is the state transition matrix, $\mathbf{U}_k$ is the accelerated velocity matrix of the robot, and $\mathbf{B}$ is the

correlation matrix between $\mathbf{U}_k$ and $\mathbf{X}_k$. $\mathbf{W}_k$ and $\mathbf{V}_k$ represent process and observation noise, respectively. Assuming they are independent white noises, which conform to the Gaussian distribution. $\mathbf{H}$ is observation matrix.

$$\mathbf{H} = \begin{bmatrix} 1 & 0 \\ 0 & 1 \end{bmatrix} \tag{13}$$

Based on the state equation and measurement equation of the robot, the prediction equations at time k can be formulated as follows:

$$\mathbf{X}_k^{k+1} = \mathbf{AX}_k + \mathbf{U}_k = \begin{bmatrix} 1 & 0 \\ 0 & \Delta t \end{bmatrix} \begin{bmatrix} d_k \\ v_k \end{bmatrix} + \begin{bmatrix} a(\Delta t)^2/2 \\ a\Delta t \end{bmatrix} \tag{14}$$

$$\mathbf{P}_k^{k+1} = \mathbf{A} \cdot \mathbf{P}_k \cdot \mathbf{A}^T + \mathbf{Q} \tag{15}$$

where $\mathbf{P}_k$ is the covariance matrix, $\mathbf{Q}$ represents process noise covariance matrix, Δt is the time interval. When the robot climbs at a constant velocity, robot's accelerated velocity a is zero and $\mathbf{U}_k$ is zero.

The optimal position estimation vector at time $k+1$ of the robot is:

$$\mathbf{X}_{k+1}^{k+1} = \mathbf{X}_k^{k+1} + \mathbf{K}_k \cdot \left(\mathbf{Z}_k - \mathbf{H} \cdot \mathbf{X}_k^{k+1}\right) \tag{16}$$

$$\mathbf{K}_k = \mathbf{P}_k^{k+1} \cdot \mathbf{H}^T \cdot \left(\mathbf{H} \cdot \mathbf{P}_k^{k+1} \cdot \mathbf{H}^T + \mathbf{R}\right)^{-1} \tag{17}$$

where $\mathbf{R}$ is observed noise covariance matrix. The covariance matrix is updated by:

$$\mathbf{P}_{k+1}^{k+1} = \left(\mathbf{I} - \mathbf{K}_k \cdot \mathbf{H}\right) \cdot \mathbf{P}_k^{k+1} \tag{18}$$

By Kalman filtering, the discrete UWB positioning data will be optimally estimated and detected cable defects can be more accurately located.

5. Experiments

Fig. 7 shows the testing process of the inspection robot on one bridge cable. The robot could run stably on bridge cables through its driving components, and obtain 360-degree images of cable surfaces through cameras. The remote computer is used to receive and analyze the image data and record robot positions.
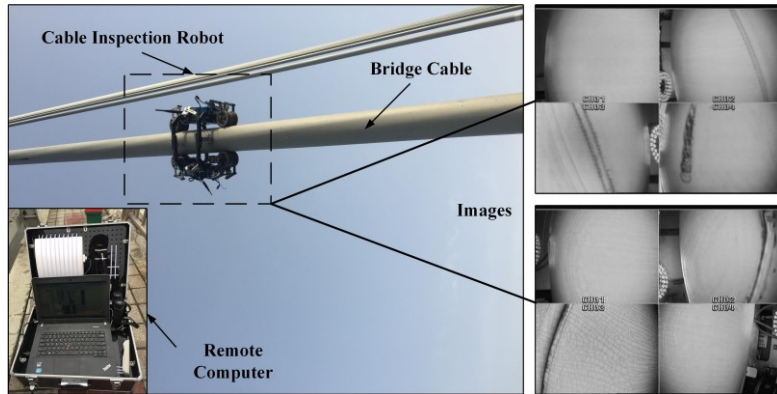
Fig. 7: Testing process of the inspection robot on a bridge cable.

5.1. Identification Experiment

The remote computer performs classification, regression, and pixel mask generation on captured cable images. The deep learning objects in the identification experiment include two categories: defect and background. The types of defects are not distinguished in detail. In our later research, more types of defects will be specifically classified.

During the identification experiment, the original images obtained by the robot were identified and predicted by Mask R-CNN. The output images were estimated defect size through a series of image

processing, mainly including background removal, filtering and binarization processing. After image processing, the proportion and size of defects in the image will be recorded and evaluated.

Fig. 8 shows the identification results of cable defect images by Mask R-CNN. The identified images include classification probability, regression box and pixel-level mask. From the experimental results, the defects in original cable images can be identified effectively, and the average probability of defect category is more than 97%. From the perspective of mask coverage, the defects in cable images are described with mask pixels completely. Compared with image processing, deep learning has the following obvious advantages:

(1) The images outside cables hardly interfere with defect identification.

(2) Defect boundary can be accurately segmented.

(3) Cable defect images are not mistakenly identified due to changes in lighting conditions.

(a) Original cable defect images

(b) Identified cable defect images
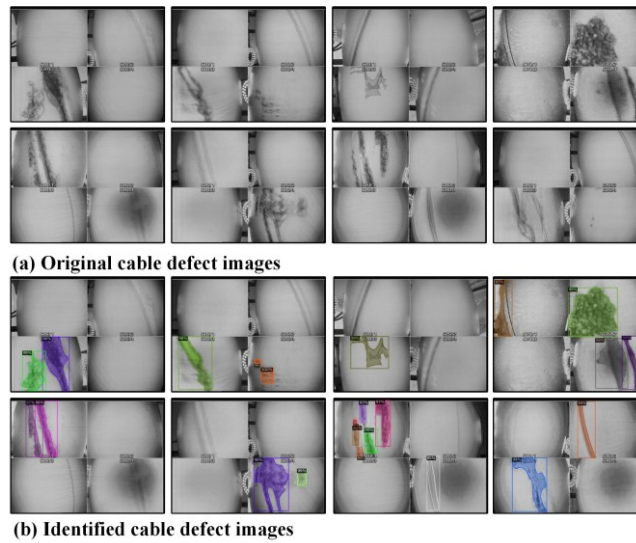
Fig. 8: Identification results of cable defects.

Some image processing algorithms, such as edge detection and change of gradient, can determine whether there are defects, but their effect is not accurate enough. By adding image processing after defect identification networks, the size of the defects can be extracted and the degree of damage can be graded. Fig. 9 shows comparative results of image processing and deep learning identification. Conventional image processing methods must filter other irrelevant things in the cable images, otherwise it will directly affect the recognition accuracy. Image processing combined with deep learning can accurately complete defect segmentation and calculation without interference from other factors.

(a) Original cable defect images

(b) Image processing results

(c) Deep learning +Image processing results
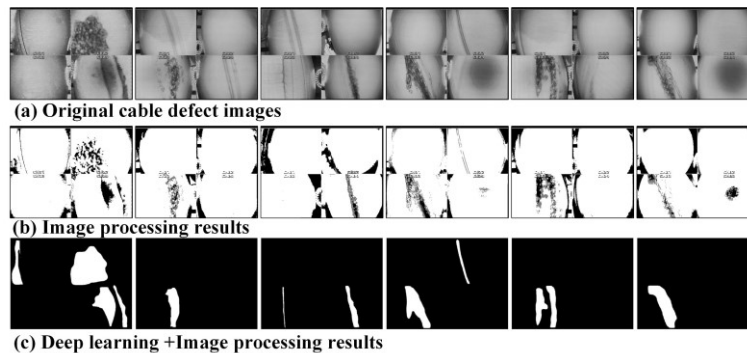
Fig. 9: Comparative results of deep learning and image processing.

Total time of cable defect identification and processing includes image loading time, identification time, image processing time. In the process of continuous image identification, the total processing time of each image is kept between 0.15 s and 0.18 s, the average identification time of each image is 0.137 s, and the

image loading loss time in real-time identification is about 0.006 s, the image processing time is about 0.0018 s.

In the real-time cable defect image identification, the robotic system can output 6 images per second. Due to the low climbing velocity of the inspection robot, it can meet the requirements of automated detection. Output speed can be improved by optimizing deep learning identification time and clearing the loss time of loading images.

5.2. Positioning Experiment

In the positioning experiment, the robot UWB tag is installed on the robot, and the UWB anchor is installed on the bottom of the cable. The final measured data is the distance from the robot to the cable bottom, and it is also used as the real-time position of the cable image.

Fig. 10 shows UWB positioning data estimated by Kalman filter when the robot was docked on the cable. The actual measurement distance is 2.5 m, and original UWB positioning data fluctuates between 2.46m and 2.56 m, with an error of ±0.05 m. After the optimized estimation by Kalman filter, the robot positioning error is maintained at ±0.02 m. The experimental results show that Kalman filter can improve the positioning accuracy and stability of UWB positioning. In the continuous positioning experiment, the robot climbed from 2 m to 11 m, and then returned to the starting point. As shown in Fig. 11, robot positioning performance is stable throughout the running process. Processed by Kalman filter, the robot positioning data is more stable and smooth, and errors caused by robot jitter are reduced.
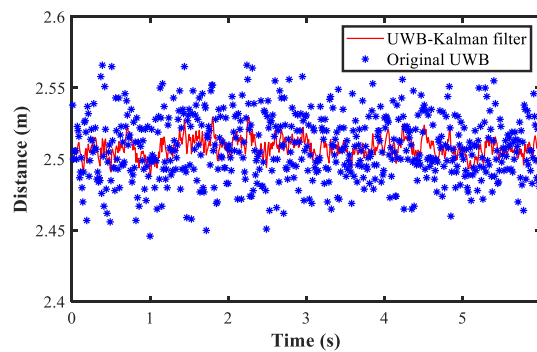
Fig. 10: UWB positioning data estimated by Kalman filter.
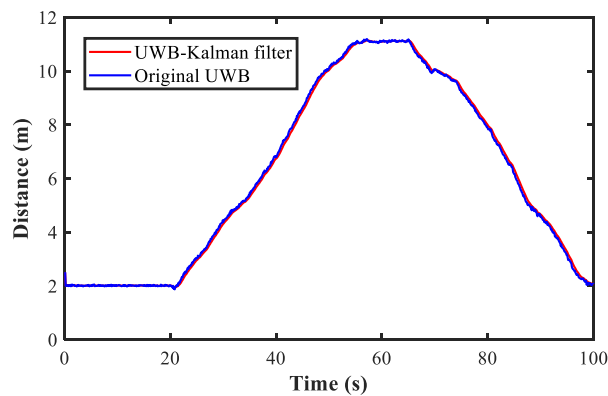
Fig. 11: Continuous positioning experiment.

6. Conclusion

This paper represents an intelligent robotic system for bridge cable defect identification and positioning. The inspection robot with elastic suspension mechanisms can stably climb on bridges cables, and obtain 360-degree images of cable surfaces through four cameras located around. By using deep learning networks, the robot can quickly identify and extract cable defects from original images. Deep learning networks consist of a series of convolutional neural networks, which can accomplish the classification, regression, and pixel-level mask generation of cable defect images. The robot can identify each cable image with processing speed

of 0.16 s, and the positions of cable defects are determined UWB positioning components. Estimated by Kalman filter, robot positioning data are more stable and accurate.

7. Acknowledgements

8. References

[1] K. H. Cho et al., "Inspection robot for hanger cable of suspension bridge: Mechanism design and analysis," vol. 18, no. 6, pp. 1665-1674, 2013.

[2] H.-B. Yun, S.-H. Kim, L. Wu, and J.-J. J. T. S. W. J. Lee, "Development of inspection robots for bridge cables," vol. 2013, 2013.

[3] X. Li, C. Gao, Y. Guo, F. He, Y. J. O. Shao, and L. Technology, "Cable surface damage detection in cable-stayed bridges using optical techniques and image mosaicking," vol. 110, pp. 36-43, 2019.

[4] K. Simonyan and A. J. a. p. a. Zisserman, "Very deep convolutional networks for large-scale image recognition," 2014.

[5] K. He, X. Zhang, S. Ren, and J. Sun, "Identity mappings in deep residual networks," in European conference on computer vision, 2016, pp. 630-645: Springer.

[6] S. Ren, K. He, R. Girshick, and J. Sun, "Faster r-cnn: Towards real-time object detection with region proposal networks," in Advances in neural information processing systems, 2015, pp. 91-99.

[7] M. Segura, H. Hashemi, C. Sisterna, and V. Mut, "Experimental demonstration of self-localized ultra wideband indoor mobile robot navigation system," in 2010 International Conference on Indoor Positioning and Indoor Navigation, 2010, pp. 1-9: IEEE.

[8] E. Takeuchi, A. Elfes, and J. Roberts, "Localization and place recognition using an ultra-wide band (uwb) radar," in Field and service robotics, 2015, pp. 275-288: Springer.

[9] A. Benini, A. Mancini, S. J. J. o. I. Longhi, and R. Systems, "An imu/uwb/vision-based extended kalman filter for mini-uav localization in indoor environment using 802.15. 4a wireless sensor network," vol. 70, no. 1-4, pp. 461-476, 2013.

[10] Q. Zhang, Y. J. S. Zhou, and I. Engineering, "Investigation of the applicability of current bridge health monitoring technology," vol. 3, no. 2, pp. 159-168, 2007.

[11] K. He, G. Gkioxari, P. Dollár, and R. Girshick, "Mask r-cnn," in Proceedings of the IEEE international conference on computer vision, 2017, pp. 2961-2969.

[12] R. Girshick, "Fast r-cnn," in Proceedings of the IEEE international conference on computer vision, 2015, pp. 1440-1448.

[13] T.-Y. Lin, P. Dollár, R. Girshick, K. He, B. Hariharan, and S. Belongie, "Feature pyramid networks for object detection," in Proceedings of the IEEE conference on computer vision and pattern recognition, 2017, pp. 2117-2125.

[14] J. Long, E. Shelhamer, and T. Darrell, "Fully convolutional networks for semantic segmentation," in Proceedings of the IEEE conference on computer vision and pattern recognition, 2015, pp. 3431-3440.

[15] P. Pettinato, N. Wirström, J. Eriksson, and T. Voigt, "Multi-channel two-way time of flight sensor network ranging," in European Conference on Wireless Sensor Networks, 2012, pp. 163-178: Springer.

[16] H. J. I. C. l. Kim, "Double-sided two-way ranging algorithm to reduce ranging time," vol. 13, no. 7, pp. 486-488, 2009.